Int. J. Heat Mass Transfer. Vol. 27, No. 8, pp. 1141–1148, 1984
Printed in Great Britain

0017-9310/84 $3.00 + 0.00
Pergamon Press Ltd.

LIQUID MIXTURES SEPARATION IN A FREEZING-OUT PROCESS

LEON GRADOŃ and DARIUSZ ORLICKI
Chemical Engineering Institute, Warsaw Technical University, Poland

(*Received* 5 *July* 1982 *and in revised form* 21 *February* 1983)

Abstract—In this paper we present a mathematical model for freezing out a component from a bicomponent alloy that forms a eutectic. The model takes into account the change of physicochemical parameters of the process with time and freezing-out space and the occlusion phenomena on the phase boundary. From the numerical solution the effect of the process parameters on the efficiency of separation measured by the separation coefficient can be determined.

NOMENCLATURE

C	molar concentration [mol l^{-1}]
c_p	specific heat [J kg^{-1} K^{-1}]
D	diffusion coefficient [m^2 s^{-1}]
H	heat of solidification [J kg^{-1}]
h	integration step
K	separation coefficient, C_s/C_l [dimensionless]
T	temperature [K]
t	time [s]
u	rate of solidification [m s^{-1}]
v	rate in the liquid alloy [m s^{-1}]
x	spatial coordinate
y	mole fraction [dimensionless].

Greek symbols

α	occlusion coefficient [dimensionless]
δ	boundary layer thickness [m]
λ	thermal conductivity [W m^{-1} K^{-1}]
μ	viscosity [Pa s]
ρ	mass density [kg m^{-3}].

Subscripts

K	benzoic acid
l	liquid
N	naphthalene
s	solid.

INTRODUCTION

THE PHENOMENA of composition separation during the state of aggregation change is widely used in many processes. This separation effect occurs in the solidification of liquid mixtures, and it is applied in zone melting and freezing-out processes. Zone melting is a type of fractional crystallization process. It was described by Pfann [1]. Freezing-out processes are connected with removing liquid mixture components during cooling. The components pass across to the solid phase in a zone where the temperature is reduced. Freezing-out methods, although seldom used, are interesting because of their possible applications in the food, plastics, varnishes, and pharmacy industries among many others. Nowadays we know some different technical solutions of the freezing-out process. One of the most simple and often used methods is the separation of mixtures in so-called rotary drum freezers. The solid phase settles on the surface of a cooled drum plunged in the liquid alloy. Knowledge of its quantitative and qualitative behaviour has fundamental importance for technical applications of this process. In the case of drum freezers it is connected with defining the effectiveness and efficiency of the separation process. The efficiency is determined by the thickness of the solid phase settling on the drum layer.

Experimental studies by Chaty [2], Hayakawa *et al.* [3] and Gradoń [4] gave the basis for determining the effect of some of the parameters of the freezing-out process, so we can make the following conclusions:

(a) molten mixture mixing intensity growth causes better separation but the thickness of the frozen-out layer decreases;

(b) cooling medium temperature growth causes better separation and decreases the thickness of the solid phase layer;

(c) there exists an optimal range of mixture temperatures connected with crystallization equilibrium, for this range the separation is the best;

(d) the solid phase layer thickness depends insignificantly on the admixture concentration, the admixture effect depends on the degree of separation.

We cannot determine the effect of all the parameters on the process on the basis of experimental studies, so we have to solve the problem by constructing an adequate mathematical model of the analysed phenomena.

In 1889 Stefan in his work *The Soil Freezing* presented and analysed the following two problems (known as Stefan problems).

(1) The two-phase medium (liquid and solid) fills the space $x > 0$. Heat transport occurs by conduction only. At first the system temperature is constant $T_2 > 0$. The surface temperature at $x = 0$ is constant $T_1 < 0$ and there occurs an isothermal crystallization at the temperature $T = 0$. The process goes on without supercooling and the volume effect is negligible.

(2) The conducting medium fills the space $-\infty < x$

$< \infty$. At first the liquid phase temperature is $T_2 > 0$. The liquid phase fills the space $0 < x < \infty$. The other conditions stand as in problem (1). In both cases we should determine the temperature distribution $T_1(x, t)$ and $T_2(x, t)$ and the phase separation boundary location $x = y(t)$. The first method to solve Stefan's problem was made by Brilius in 1931. He tried to reduce this problem by solving a system of nonlinear differential equations. That way of treatment turned out to be wrong even now, as the analytical methods are developed. We know partial and asymptotical solutions that only give us simplifications of real conditions.

For a practical description of the freezing-out process in liquid alloys, taking into account the equilibrium on the phase separation surface, we can use the following simplifications:

(a) in the so-called two-phase Stefan problem we assume that physicochemical parameters are constant in the liquid and solid phases, we neglect the mass density change during the phase change. We assume also, that mass and heat is propagated by diffusion and molecular conduction [5];

(b) we widen the previous model (diffusion in the boundary layer in the liquid phase) assuming constant concentration on the phase boundary and constant rate of the crystallization front shifting [6];

(c) we assume a linear distribution of concentration in the liquid phase boundary layer, the pressure change on the phase separation surface and the change in the rate of the crystallization front [7].

Other published works modify the above drifts only slightly. Most of the results of the engineering problems obtained in this way can be applied only for a quantitative estimation. These results cannot establish the basis for analysing the process.

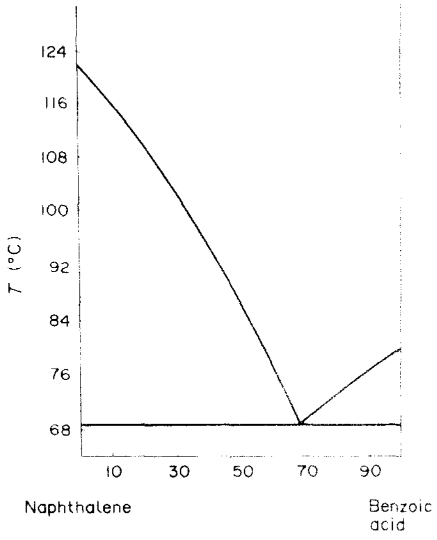

FIG. 2. Crystallization equilibrium for naphthalene–benzoic acid mixture.

MATHEMATICAL DESCRIPTION OF THE PROCESS

In a sink with a mixer (Fig. 1) we have a bicomponent alloy. The liquid phase core temperature is T_∞ and the frozen-out component concentration is C_∞. In this sink is also a turning barrel with a wall temperature T_0. For making computations we analyse a naphthalene–benzoic acid system that forms a eutectic. Figure 2 shows the crystallization equilibrium curve for this system. Figure 3 presents an illustration of the physical conditions of the model. Our mathematical model was derived on the basis of the following assumptions:

(a) the barrel radius is much bigger than the boundary layer thickness, so we can treat this problem as one-dimensional;

(b) the crystallization centres are uniformly arranged on the interface, the quantity of centres is satisfactory;

(c) there is a local thermodynamical equilibrium on the interface;

(d) we neglect the thermodynamical effects and the components' diffusion in the solid phase;

(e) we neglect the pressure gradient and energy dissipation;

(f) external fields do not affect the system.

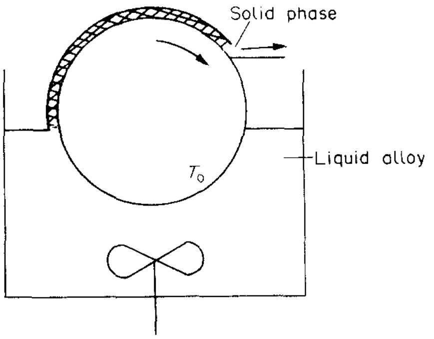

FIG. 1. Outline of freezing-out system.

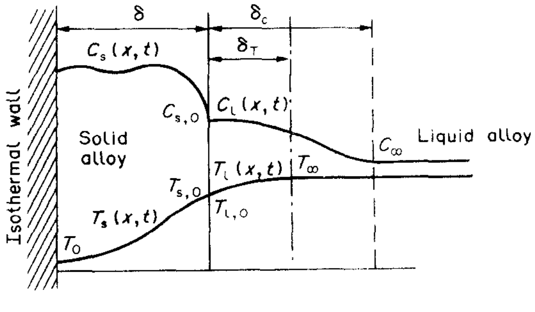

FIG. 3. Physical conditions of the solidification process for a bicomponent alloy—an illustration.

The model regards the change in physicochemical parameters during freezing out and the occlusion on the interface.

Mass, momentum and energy balances were determined on the basis of the boundary layer model in the inertia coordinate system connected with the interface.

The basis for all of the balances presented below is the time period Δt. Uniform surfaces S normal to the x-direction have a distance Δx (Fig. 4). We will present final results of the mass and energy balances and the boundary and initial conditions for each of these equations. Subscripts l and s stand for the liquid phase and the solid phase, respectively. Where double subscripts are used the second subscript N or K stands for naphthalene or benzoic acid.

MASS TRANSPORT EQUATION IN THE SOLID PHASE

$$-u(t)\frac{\partial C_{s,N}(x,t)}{\partial x}+\frac{\partial C_{s,N}(x,t)}{\partial t}=0, \quad (1a)$$

$$C_{s,N}(x,0)=0, \quad (1b)$$

$$C_{s,N}(0,t)=C_{s,0}(t). \quad (1c)$$

ENERGY TRANSPORT EQUATION IN THE SOLID PHASE

According to the assumptions made earlier, the energy transport occurs only by convection and conduction. The final equation is

$$-\frac{\partial}{\partial x}\left(\lambda_s(x,t)\frac{\partial T_s(x,t)}{\partial x}\right)$$
$$-u(t)\frac{\partial}{\partial x}(\rho_s(x,t)c_{ps}(x,t)T_s(x,t))$$
$$+\frac{\partial}{\partial t}(\rho_s(x,t)c_{ps}(x,t)T_s(x,t))=0, \quad (2a)$$

$$T_s(0,0)=T_0, \quad (2b)$$

$$T_s(0,t)=T_K(t), \qquad T_s(-u(t)t,t)=T_0. \quad (2c)$$

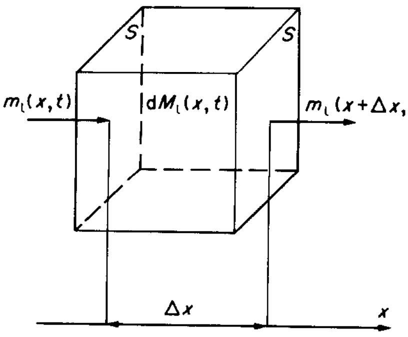

FIG. 4. Control volume for mass balance.

MASS TRANSPORT EQUATION IN A LIQUID ALLOY

The equation contains some elements of diffusion and convection. The convection flux rate is $V(x,t)$. This parameter value and its definition is given below

$$-\frac{\partial}{\partial x}\left(D_{N,K}(x,t)C_l(x,t)\frac{\partial y_N(x,t)}{\partial x}\right)$$
$$+\frac{\partial}{\partial x}(V(x,t)C_{l,N}(x,t))+\frac{\partial C_{l,N}(x,t)}{\partial t}=0, \quad (3a)$$

$$C_{l,N}(x,0)=C_\infty, \quad (3b)$$

$$C_{l,N}(0,t)=C_{l,0}(t), \qquad C_{l,N}(\delta_c,t)=C_\infty, \quad (3c)$$

where

$$y_N(x,t)=\frac{C_{l,N}(x,t)}{C_{l,N}(x,t)+C_{l,K}(C_{l,N},T_l)}.$$

ENERGY TRANSPORT EQUATION IN A LIQUID ALLOY

$$\frac{\partial}{\partial x}\left(\lambda_l(x,t)\frac{\partial T_l(x,t)}{\partial x}\right)$$
$$+\frac{\partial}{\partial x}(V(x,t)\rho_l(x,t)c_{pl}(x,t)T_l(x,t))$$
$$-\frac{\partial}{\partial x}\left(D_{N,K}(x,t)C_l(x,t)M_N c_{pl,N}(x,t)T_l(x,t)\right.$$
$$\left.\times\frac{\partial}{\partial x}y_N(x,t)\right)$$
$$-\frac{\partial}{\partial x}\left(D_{K,N}(x,t)C_l(x,t)M_K c_{pl,K}(x,t)T_l(x,t)\right.$$
$$\left.\times\frac{\partial}{\partial x}y_K(x,t)\right)$$
$$+\frac{\partial}{\partial t}(\rho_l(x,t)c_{pl}(x,t)T_l(x,t))=0, \quad (4a)$$

$$T_l(x,0)=T_\infty, \quad (4b)$$

$$T_l(0,t)=T_K(t), \qquad T_l(\delta_t,t)=T_\infty. \quad (4c)$$

CONTINUITY EQUATION IN A LIQUID ALLOY

$$\frac{\partial}{\partial x}(\rho_l(x,t)V(x,t))$$
$$-\frac{\partial}{\partial x}\left(D_{N,K}(x,t)C_l(x,t)M_N\frac{\partial}{\partial x}y_N(x,t)\right)$$
$$-\frac{\partial}{\partial x}\left(D_{K,N}(x,t)C_l(x,t)M_K\frac{\partial}{\partial x}y_N(x,t)\right)$$
$$+\frac{\partial}{\partial t}(\rho_l(x,t))=0, \quad (5a)$$

with the boundary condition

$$V(0,t)=-u(t)+f(x,t)u(t). \quad (5b)$$

The first term of the sum in equation (5a) is connected with analysing the process in a moving coordinate system, while the second term represents the rate of liquid movement caused by the change in mass density during the phase change. We calculate the function $f(x, t)$ on the basis of a simple differential balance. We assume that during the time period, Δt, the liquid volume changes, ΔV_l, into the solid phase volume, ΔV_s. The function $f(x, t)$ is given as

$$f(x,t) = 1 - \frac{\rho_s(x,t)}{\rho_l(x,t)}.$$

DIFFERENTIAL MASS BALANCE ON THE INTERFACE

$$-u(t)C_{s,N}(0,t) - V(0,t)C_{l,N}(0,t)$$

$$+ D_{N,K}(0,t)C_l(0,t)\frac{\partial}{\partial x}y_N(x,t)|_{x=0} = 0. \quad (6a)$$

Moreover

$$C_{s,N}(0,t) = C_{s,0}(t), \qquad C_{l,N}(0,t) = C_{l,0}(t).$$

We can determine $C_{s,0}(t)$ and $C_{l,0}(t)$ values on the crystallization surface for a given time and a given temperature, T_K, from the crystallization equilibrium curve; for $C_{s,0}(t)$ we take into account the occlusion phenomena

$$C_{l,0}(t) = f_l(T_K(t)), \quad (6b)$$

$$C_{s,0}(t) = (1-\alpha(t))f_s(T_K(t)) + \alpha(t)f_l(T_K(t)). \quad (6c)$$

The crystallization equilibrium curve shown in Fig. 3 was approximated by second-order polynomials [$f_l(T)$ and $f_s(T)$] using the least squares method.

We define the occlusion coefficient, α, as a frozen-out volume fraction filled with a liquid phase closed among crystals of the dendritic form. This coefficient is also the crystallization ratio function. The definition of $\alpha(t)$ is given below.

DIFFERENTIAL ENERGY BALANCE ON THE INTERFACE

$$-\lambda_s(0,t)\frac{\partial}{\partial x}T_s(x,t)|_{x=0}$$

$$-u(t)\rho_s(0,t)c_{ps}(0,t)T_s(0,t)$$

$$+\lambda_l(0,t)\frac{\partial}{\partial x}T_l(x,t)|_{x=0}$$

$$-v(t)\rho_l(0,t)c_{pl}(0,t)T_l(0,t)$$

$$+D_{N,K}(0,t)C_l(0,t)M_N c_{pl,N}(0,t)T_l(0,t)$$

$$\times\frac{\partial}{\partial x}y_N(x,t)|_{x=0}$$

$$+D_{K,N}(0,t)C_l(0,t)M_K c_{pl,N}(0,t)T_l(0,t)$$

$$\times\frac{\partial}{\partial x}y_K(x,t)|_{x=0} - u(t)\rho_s(0,t)H(t) = 0, \quad (7a)$$

$$T_s(0,t) = T_K(t), \qquad T_l(0,t) = T_K(t). \quad (7b)$$

DEFINITION OF THE PROCESS PARAMETERS OCCURRING IN THE MATHEMATICAL DESCRIPTION

For solving the problem formulated by the equations system, equations (1)–(7), we must know the physicochemical properties of the system, mainly the parameters occurring in the equations system as functions of concentration and temperature.

To determine these functions we use literature data [8] and our own experimental data [9]. The numerical data were approximated by polynomials of the necessary order using the least squares method. In the case of a lack of numerical values we used correlations. The final analytical correlation functions are nonlinear and complicated, so we present only the origin of the correlation.

(1) *The diffusion coefficient* for the liquid component is calculated according to Wilke's method [10], the mass density as a temperature function gives the Andrade formula [11].

(2) *The liquid phase heat conduction coefficient* was determined using Filippov and Novosielova's method [12]; the conduction coefficient for the pure component was calculated using Rabbius and Kinger's method.

(3) *The heat of phase transition* as a temperature function was determined from the following equation

$$\frac{dH}{dT} = \Delta c_p + \frac{H}{T} - \frac{H}{\Delta V}\left(\frac{d\Delta V}{dT}\right)_p,$$

where

$$\Delta c_p = c_{pl} - c_{ps},$$

and

$$\Delta V = V_l - V_s.$$

(4) *Boundary layer thickness.* The energy balance on the interface [equation (7a)], while the solid phase layer thickness is maximal [$V(0,t) = 0$], is

$$-\lambda_s(0,t)\frac{\partial T_s(x,t)}{\partial x}\bigg|_{x=0} + \lambda_l(0,t)\frac{\partial T_l(x,t)}{\partial x}\bigg|_{x=0} = 0. \quad (8)$$

The temperature distribution in the solid material thermal boundary layer can be treated as linear, as was confirmed during computations if time is sufficiently long

$$-\lambda_s(0,t)\frac{T_K(t) - T_0}{\delta_{max}} + \lambda_l(0,t)\frac{T_\infty - T_K(t)}{\delta_t} = 0. \quad (9)$$

For long times the following assumption is admissible

$$\lim_{t\to\infty} C_l(0,t) = C \quad \text{and} \quad \lim_{t\to\infty} T_K(t) = f_l^{-1}(\infty). \quad (10)$$

Based on the analysis presented above the thermal boundary layer thickness for a given δ_{max} can be estimated. On the basis of the experimental data [9] for different hydrodynamical conditions we find, that the thickness δ_t value is in the range 5×10^{-5}–4×10^{-4} m. According to the film model of mass and heat penetration, the boundary layer thickness ratio from

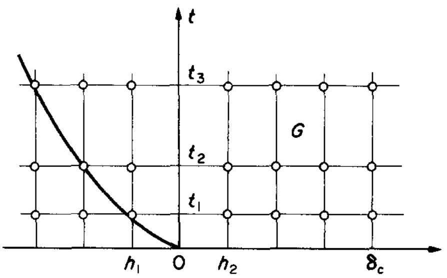

FIG. 5. Schedule for computations of equations (1)–(7).

the Chilton–Colburn correlation is given in the form

$$\frac{\delta_t}{\delta_c}=\left(\frac{\lambda_l(x,t)}{D(x,t)c_{pl}(x,t)\rho_l(x,t)}\right)^{1/3}. \tag{11}$$

(5) *The occlusion coefficient.* The occlusion phenomenon is connected with conditions and mechanisms of crystal growth. This effect is noticed when the difference of process parameters is significant, so the growth is quick. Until now we had no theoretical basis for determining the analytical form of the occlusion function. A literature analysis [4] gives the suggestion, that dendritical crystal growth is responsible for occlusion.

Langer and Müller-Krumbhaar [13–16] proposed the stability criterion for given crystal curvature under given growth conditions. The instabilities are spatially oscillating modes localized at the tip. Interferences of branches at neighbouring crystals are the reason why occlusion takes place. On the basis of their analysis and experimental studies the occlusion function is given as

$$\alpha(t)=a\exp\left(-\frac{b}{u(t)}\right), \tag{12}$$

where *a* and *b* are positive constants.

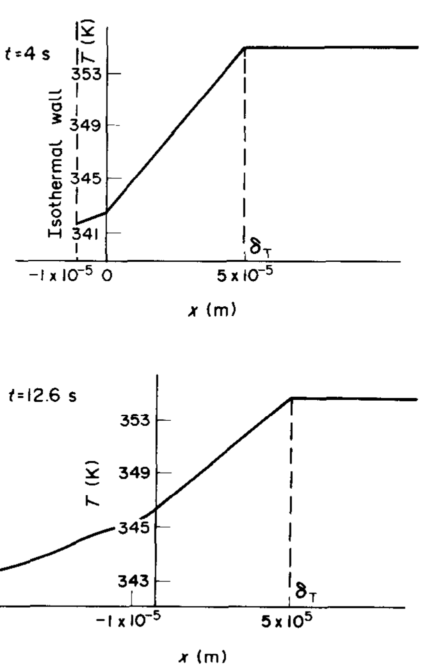

FIG. 6. Temperature distribution in a thermal boundary layer and in a solid layer for different process times.

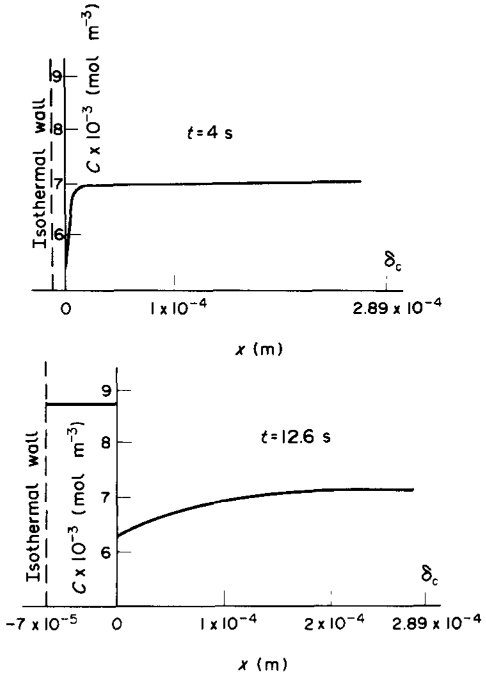

FIG. 7. Naphthalene concentration distribution in a concentration boundary layer and in a solid layer for different process times.

EQUATIONS SYSTEM, EQUATIONS (1)–(7), SOLUTION

The equations system, equations (1)–(7), with nonlinear coefficients was solved using the difference method. We applied the Crank–Nicolson method with the difference operators, Δ, and the mean differences, μ and μ^2.

The network scheme is shown in Fig. 5.

We isolate two problems connected by the balance on the interface and analyse separately the concentration and temperature distributions in the liquid and solid phases. This network enables us also to solve this

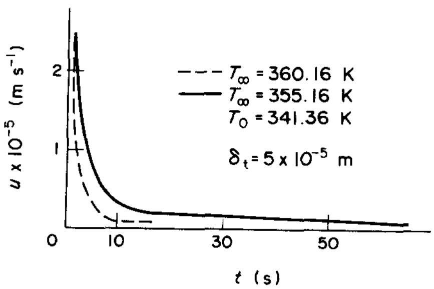

FIG. 8. The rate of solidification as a function of time.

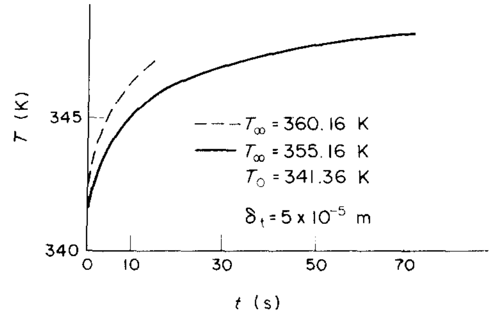

FIG. 9. Interphase surface temperature as a function of time.

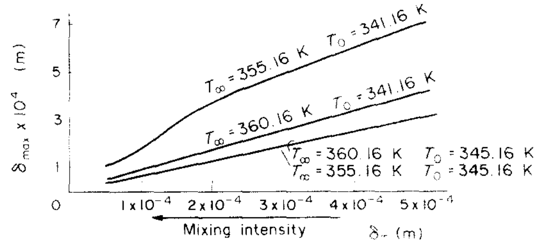

FIG. 11. Maximum solid phase layer thickness as a function of the thermal boundary layer thickness.

problem for a given solid phase thickness. The Crank–Nicolson method gives the convergence of the solution for finite values of h and $(t \cdot k)$. The stability was verified during computer experiments, so that we can reduce the differential equation system, equations (1)–(7), to the difference equation system using the above-mentioned method.

Please note that for computation of the value of functions $u(t_j)$ and $T(t_j)$ in a given moment t_j we use equations (6a) and (7a). At the moment t_j the concentration and temperature distribution near the interface is specified.

RESULTS

We present an example of computations for the following data: raw liquid mixture containing 90 wt % of naphthalene and 10 wt % of benzoic acid, liquid core temperature $T_\infty = 355.16$ and 360.16 K, and isothermal cold wall temperature $T_0 = 341.16$ and 354.16 K. The computations were made for four values of the thermal boundary layer thickness—$\delta_t = 5 \times 10^{-5}$, 1×10^{-4}, 2×10^{-4}, and 5×10^{-4} m. This wide range gives possibly the complete effect of hydrodynamical conditions on the process.

Figure 6 presents the temperature profiles in the liquid medium and in the thermal boundary layer for different process times. The real temperature distribution can be approximated at any moment by the straight line. The linear approximation for the naphthalene concentration distribution in the concentration boundary layer is permissible after long enough time (Fig. 7). The curve presenting the crystallization rate as a function of time monotonically decreases. The initial steep decrease of the rate u is caused by the temperature difference of the crystallization surface and the liquid (Fig. 8). The character of the function $u(t)$ is important for the product purity, because α is a function of $u(t)$.

Figure 9 presents the crystallization surface temperature as a function of time. It is easy to prove that there exists an asymptote T = const. which represents the temperature in which the liquid alloy becomes a saturated solution. Analysing Figs. 10–12 we can notice that:

(a) when the liquid alloy temperature grows, the maximum solid phase layer thickness and the freezing-out time decreases, the distribution coefficient increases;

(b) the cooling medium temperature growth causes a decrease of the maximum solid phase layer thickness, an increase of the distribution coefficient and a freezing-out time elongation;

(c) the mixing intensity increase causes a reduction of the maximum solid phase layer thickness, an increase of the distribution coefficient and a freezing-out time shortening.

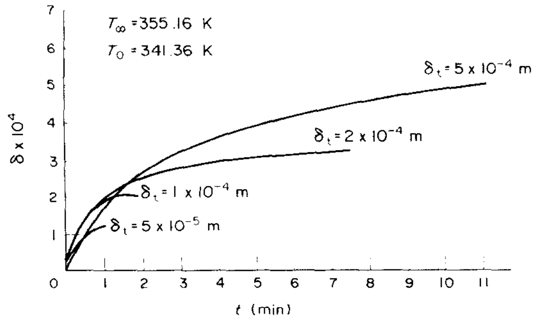

FIG. 10. Solid phase layer thickness as a function of time for different thermal boundary layer thicknesses.

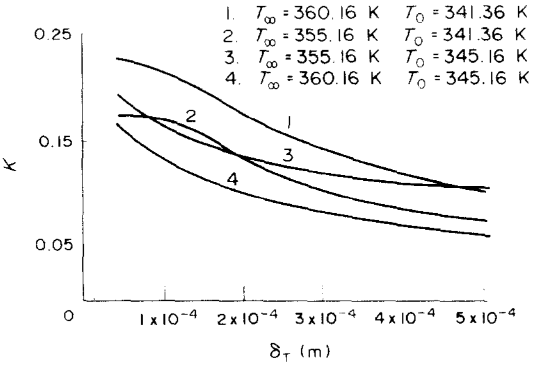

FIG. 12. Distribution coefficient as a function of the thermal boundary layer thickness.

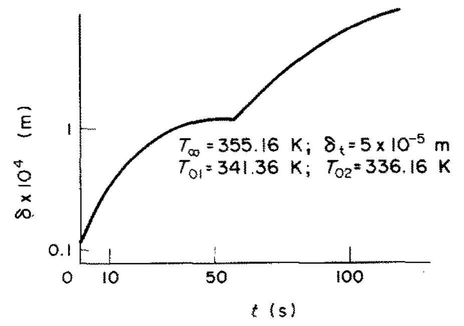

FIG. 13. Solid phase layer thickness as a function of time for a two-chamber freezer.

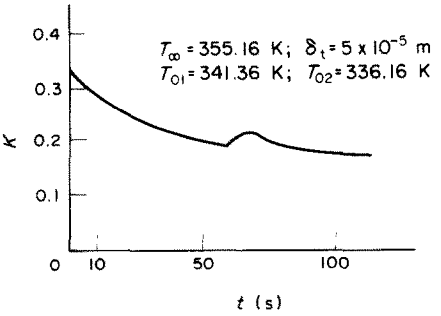

FIG. 14. Distribution coefficient as a function of time for a two-chamber freezer.

These results confirm conclusions presented in experimental works [2, 9].

Another important problem is the process intensification. In barrel freezers this is limited by the increasing solid phase layer thickness and the decreasing distribution coefficient.

Till now the solid layer thickness growth was reached by reducing the cooling medium temperature below T_1, but the final product quality was deteriorated. We suggest that the freezer is divided into sections with different cooling medium temperatures. The temperature should decrease in the direction of the barrel motion. Example computations for two-chamber freezers are presented in Figs. 13 and 14. The separation efficiency is doubled, while the distribution coefficient is comparable with the coefficient for a one section system.

REFERENCES

1. W. Pfann, *Zone Melting*. Wiley, New York (1966).
2. J. C. Chaty, Rotary drum techniques, *Fractional Solidification*, Vol. 1. Dekker, New York (1967).
3. T. Hayakawa, M. Matsouka and K. Satake, Phenomena of solidification in normal freezing, *J. Chem. Engng Japan* **6**(4), 332 (1973).
4. L. Gradoń, Unpublished works (1982).
5. L. I. Rubinstein, *Probliema Stefana*. Izd. Zgwajgzne, Riga (1967).
6. J. A. Burton, R. C. Prim and W. P. Slichtor, The distribution of solute in crystal grown from the melt, *J. Chem. Phys.* **21**, 1987 (1953).
7. R. Wasiak, M. thesis, Warsaw Technical University, Warsaw (1978).
8. R. H. Perry and C. H. Chilton, *Chemical Engineers Handbook* (Vth edn.). McGraw-Hill, New York (1974).
9. E. Płóciennik, Ms. thesis, Warsaw Technical University, Warsaw (1980).
10. C. R. Wilke, Estimation of liquid diffusion coefficients, *Chem. Engng Prog.* **45**, 218 (1949).
11. E. C. Andrade, A theory of the viscosity of liquids, *Phil. Mag.* **17**, 457 (1934).
12. L. P. Filippov and N. L. Novosielova, Tieploprovodnost rastvorov normalnych żidkostiej, *Westnik Moskowskovo Univ.* **10**, 3 (1955).
13. H. Müller-Krumbhaar and J. S. Langer, Theory of dendritic growth, I. Elements of a stability analysis, *Acta Metall.* **26**, 1681 (1977).
14. H. Müller-Krumbhaar and J. S. Langer, Theory of dendritic growth, II. Instabilities in the limit of vanishing surface tension, *Acta Metall.* **26**, 1689 (1977).
15. H. Müller-Krumbhaar and J. S. Langer, Sidebranching instabilities in a two-dimensional model of dendritic solidification, *Acta Metall.* **29**, 145 (1981).
16. J. S. Langer, Dendritic solidification of dilute solutions, *PhysicoChemical Hydrodynamics* **1**, 44 (1980).

SÉPARATION DES MÉLANGES LIQUIDES PAR CONGELATION

Résumé—Le travail represente le modele mathematique de la frigelisation du composant en alliage binaire formant un eutectique simple. Le modele prend en consideration le changement des parametres physico-chimiques du processus en temps et espace de frigelisation ainsi que le phenomene de l'occlusion sur l'interphase. La solution numerique du modele definit l'influence des conditions du processus sur son efficacite exprimee par le coefficient de separation.

DIE TRENNUNG VON FLÜSSIGKEITSGEMISCHEN IN EINEM AUSFRIER-PROZEß

Zusammenfassung—In vorliegender Arbeit wurde das mathematische Modell des Ausfrierens einer Komponente aus der Zweikomponenten-Schmelze mit einem eutektischen Punkt untersucht. In dem Modell wurden die Zeit- und Raumänderungen von physikalisch-chemischen Parametern sowie die an der Phasengrenze auftretende Okklusion berücksichtigt. Aus der numerischen Lösung des Modells lässt sich der Einfluss von Prozess-bedingungen auf die durch den Verteilungskoeffizienten ausgedrückte Trennwirkung des Ausfrierens bestimmen.

РАЗДЕЛЕНИЕ СМЕСЕЙ ЖИДКОСТЕЙ В ПРОЦЕССЕ ВЫМОРАЖИВАНИЯ

Аннотация—Предложена математическая модель процесса вымораживания одной из компонент двухкомпонентного эвтектического сплава. Модель учитывает изменение во времени физикохимических параметров процесса, области вымораживания, а также окклюзии на границе раздела фаз. Численным решением определено влияние параметров процесса на эффективность разделения, определяемую коэффициентом разделения.